Title

Activation of YAP attenuates hepatic damage and fibrosis in liver ischemia-reperfusion injury.

Permalink

https://escholarship.org/uc/item/88b850v4

Journal

Journal of hepatology, 71(4)

ISSN

0168-8278

Authors

Liu, Yuan
Lu, Tianfei
Zhang, Cheng
et al.

Publication Date

2019-10-01

DOI

10.1016/j.jhep.2019.05.029

Peer reviewed

Activation of YAP Attenuates Hepatic Damage and Fibrosis in Liver Ischemia-Reperfusion Injury

Yuan Liu[1,2,*], **Tianfei Lu**[1,2,*], **Cheng Zhang**[1,3,*], **Jin Xu**[1,4], **Zhengze Xue**[1,3], **Ronald W. Busuttil**[1], **Ning Xu**[2], **Qiang Xia**[2], **Jerzy W. Kupiec-Weglinski**[1], **Haofeng Ji**[1]

[1]Dumont-UCLA Transplant Center, Division of Liver and Pancreas Transplantation, Department of Surgery, David Geffen School of Medicine at University of California-Los Angeles, Los Angeles, CA, USA

[2]Department of Liver Surgery, Ren Ji Hospital affiliated to Shanghai Jiao Tong University School of Medicine, Shanghai, China

[3]Department of Surgery, Division of Hepatobiliary and Pancreatic Surgery, The First Affiliated Hospital, Zhejiang University, School of Medicine, Hangzhou, Zhejiang, China

[4]Department of Pancreatic Surgery, Shengjing Hospital, China Medical University, Shenyang, China

Abstract

Background & Aims: Hepatic ischemia-reperfusion injury (IRI) is a major complication of hemorrhagic shock, liver resection and transplantation. YAP, the effector of Hippo pathway, is essential in determining cell fate and maintaining homeostasis in the liver.

Methods: This study systemically evaluated putative role of YAP/Hippo signaling in human orthotopic liver transplantation (OLT) and in a murine model of liver warm IRI.

Results: Hepatic biopsy specimens from OLT patients (n=60) were collected after 2-10h of cold storage (pre-OLT) and 3h post-reperfusion (post-OLT) under an institutional research broad protocol, and screened by Western blots. High post-OLT YAP expression was correlated with well-preserved histology and improved hepatocellular function at post-operative day 1-7 (POD 1-7). In mice, the ischemia insult (90min) triggered intrinsic hepatic YAP expression, peaking at 1-6h of reperfusion. Activating YAP protected liver against IR-stress, promoted downstream regenerative/anti-oxidative gene induction, diminished oxidative stress and necrosis/apoptosis, and suppressed

Conflict of interest statement: The authors declare no conflicts of interest that pertain to this work.

innate inflammation response. In contrast, inhibiting YAP aggravated hepatic IRI and suppressed repair/anti-oxidative genes. In parallel *in vitro* studies, activating YAP prevented hypoxia-reoxygenation induced stress in mouse hepatocyte cultures. Although sALT levels were progressively decreased from 6h to 7d post-reperfusion in IR-stressed mouse livers, hepatic fibrogenesis was steadily developing. Interestingly, YAP activation suppressed extracellular matrix synthesis and diminished hepatic stellate cells (HSCs) activation, whereas YAP inhibition significantly delayed hepatic repair, potentiated HSCs activation, and enhanced liver fibrosis at 7d post-IRI. However, YAP activation failed to protect Nrf2-deficient livers against IR-mediated damage, leading to extensive fibrosis.

Conclusion: Our novel findings document the crucial role of YAP in IR-mediated hepatocellular damage and liver fibrogenesis, and imply the therapeutic potential for the management of sterile liver inflammation in transplant recipients.

Lay summary:

In the clinical arm, graft YAP expression negatively correlated with liver function and tissue damage in human OLT. We then demonstrated that YAP activation attenuated hepatocellular oxidative stress and diminished innate immune response in mouse liver IRI. YAP inhibited HSCs activation, and abolished IR-mediated mouse liver fibrogenesis during 7d post-IRI. However, YAP activation failed to prevent IR-injury in Nrf2-deficient livers damage, leading to extensive fibrosis.

Graphical Abstract
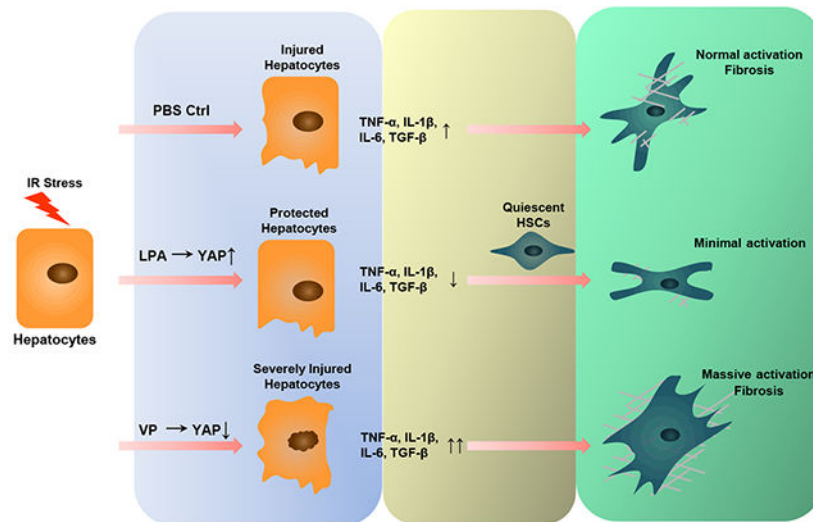
Keywords

Fibrosis; Liver Ischemia-Reperfusion Injury; Orthotopic Liver Transplantation; YAP

Introduction

Orthotopic liver transplantation (OLT) is considered as the standard treatment for end-stage liver disease. Resulting from organ retrieval, cold preservation and warm ischemia-

reperfusion injury (IRI) can lead to impaired graft function up to and including primary graft non-function, which may predispose to acute and chronic rejection. Indeed, by contributing to a shortage of available donor organs, IRI represents one of the most challenging problems in transplantation[1–4]. Thus, novel therapeutic concepts to combat IRI are needed to improve OLT outcomes and expand donor organ pool.

Hepatic IRI, initiated by hypoxia stress, is an exogenous antigen-independent local inflammation response. IR-insulted hepatocytes then produce damage-associated molecular patterns, which trigger innate immune responses and inflammation[3]. Hepatocellular death is mainly featured as hypoxia-reactive oxygen species (ROS) induced hepatocellular necrosis and innate pro-inflammatory cytokines mediated apoptosis in liver IRI[2].

Liver fibrosis is a highly conserved and coordinated protective response to tissue injury, which disrupts the normal liver architecture, and causes hepatocellular dysfunction and portal hypertension[5–8]. Hepatic stellate cells (HSCs) are considered the major source of liver myofibroblasts[9–11]. The interaction between macrophage-mediated innate immunity and HSCs activation/proliferation is essential in liver fibrogenesis[12–14]. Prolonged ischemia time was considered as one of the most important risk factors related to post-transplant hepatic fibrosis in pediatric liver transplantation[7]. However, the mechanism of IR-mediated fibrosis/cirrhosis and chronic graft non-function remains to be determined.

The Hippo pathway and its downstream effector YAP (Yes-associated protein) control organ size in animals through the regulation of cell proliferation and apoptosis[15,16]. Hippo signaling sequesters YAP to the cytoplasm via phospho-specific and cell-tension based mechanisms[17]. YAP primarily binds to the TEAD family of transcription factors to activate target gene expression[17]. In mammalian liver, YAP determines cell fate and maintaining homeostasis[18]. Its high-to-low gradient expression from portal vein area to central vein contributes to the heterogeneity of hepatocytes and liver zonation[19,20]. Loss of YAP in the liver leads to defects in both hepatocyte survival and biliary epithelial cell development[21], whereas its ectopic activation results in hepatocyte dedifferentiation and hepatomegaly, and may promote carcinogenesis[15,16,22]. After hepatectomy, YAP activation was also found essential for liver repair and regeneration[23,24].

Here, we evaluated the role of YAP/Hippo pathway in hepatocellular protection and hepatic fibrosis induction during liver IRI. This study examined as to whether and how YAP signaling may affect hepatocyte function, innate immune response, and HSCs mediated tissue repair/fibrosis in well-established murine liver IRI model. Our clinical arm reinforced the pivotal role of YAP in hepatocellular protection in human OLT. By providing evidence for previously unrecognized role of YAP in hepatic protection, repair/regeneration, and fibrosis, this study provides new insights into the potential therapeutic intervention against sterile inflammatory liver injury and fibrosis.

Materials and Methods

Clinical liver transplantation study.

Sixty adult OLT recipients were recruited under an institutional research board protocol (#ChiCTR-IIR-16008040: March 2018-November 2018, Ren Ji Hospital, Shanghai, China). All organ donations recorded in the electronic database were contributed voluntarily, and no donor organs were obtained from executed prisoners or other institutionalized persons. Informed consent was obtained from all subjects. Routine standard pre-OLT evaluation and immunosuppression therapy were administered. Non-fatty donor organs, procured according to standardized techniques, were perfused with and stored in cold University of Wisconsin (UW) solution. Cold ischemia time was defined as the time between the perfusion of the donor liver with UW solution and its removal from the cold storage. Hepatocellular injury was evaluated by serum alanine aminotransferase (sALT) at postoperative days (PODs) 1-7. Liver biopsies were obtained from the left lobe during back-table preparation (pre-OLT: prior to implantation), and at 3h after portal reperfusion (post-OLT: prior to the abdominal closure).

Mouse warm liver IRI model.

Male 6-8 weeks old wild-type (WT) mice (Jackson Laboratory, Bar Harbor, ME) or Nrf2-deficient mice (breeding pairs provided by Dr. Thomas Kensler, Johns Hopkins University) on a C57BL/6 background (backcrossed for at least 12 generations) were used in a model of partial warm hepatic IR, as described[1-3]. In general, the arterial/portal vessels to the cephalad lobes were clamped for 90min. No vascular occlusion in sham-controlled mice. In the treatment groups, animals were infused at 1h prior to the onset of liver ischemia with a single dose of YAP activator (1-oleoyl lysophosphatidic acid (LPA): 0.8μmol/kg i.v., Tocris Bioscience, Minneapolis, MN) or YAP inhibitor (verteporfin (VP): 0.8pmol/kg i.v., MilliporeSigma, St. Louis, MO) dissolved in PBS. Mice were sacrificed at various time-points after reperfusion; liver and serum samples were collected for analysis. All animal experiments were approved by UCLA Animal Research Committee.

ALT Measurement.

Serum and culture medium ALT levels were measured by ALT kit (ThermoFisher, Waltham, MA) according to the manufacturer's instructions.

Western blot.

Liver proteins (30μg/sample) were separated by gel electrophoresis and transferred to nitrocellulose membrane. YAP, phospho-YAP(Ser127), Nrf2 and β-actin monoclonal antibody (mAbs) (Cell Signaling Technology, Danvers, MA) were used for probe. To compare protein expression in multiple human OLT samples, densitometry quantification was conducted. The YAP protein value was normalized according to β-actin intensity.

Histopathology.

Liver specimens (5μm), stained with hematoxylin and eosin (H&E), Masson's trichrome staining and Sirius red staining were analyzed blindly. Primary mAbs against YAP (Cell

Signaling Technology), macrophages (CD68) (AbD Serotec, Raleigh, NC), neutrophils (Ly6G) (BD Biosciences, San Jose, CA), and α-SMA (Abeam, Cambridge, MA) were used. Superoxide levels in hepatic tissue were detected with ROS-sensing dye dihydroethidium (DHE; AnaSpec, Fremont, CA). Liver sections were evaluated blindly by counting labeled cells in 10 high-power fields (HPF).

Quantitative RT-PCR.

Quantitative PCR was performed with platinum SYBR green quantitative PCR kit (ThermoFisher) by the QuantStudio3 (ThermoFisher). Primers to amplify specific gene fragments were published[1"3]. Target gene expressions were calculated by their ratios to the housekeeping gene hypoxanthine-guanine phosphoribosyl transferase (HPRT).

Terminal Deoxynucleotidyl Transferase-Mediated dUTP Nick End Labeling (TUNEL) Assay.

DNA fragments in liver sections, resulting from necrosis/apoptosis, were detected by the TUNEL method (Klenow-FragEL DNA Fragmentation Detection Kit; MilliporeSigma). TUNEL-positive cells were counted in 10 HPF/section.

Hepatocyte culture.

Mouse hepatocytes were isolated by *in situ* collagenase perfusion followed by Percoll gradient centrifugation, and cultured with complete William's E medium plus maintenance supplement (ThermoFisher) for 24h. For hypoxia-reoxygenation experiment, culture medium, supplied with LPA (10μM), VP (10μM) or PBS and equilibrated in $95\%N_2$-$5\%CO_2$ or $95\%O_2$-$5\%CO_2$, was used as hypoxia or reoxygenation medium, respectively. Cells were cultured with hypoxia medium at 37°C for 6h in a humidity airtight chamber equilibrated with $95\%N_2$-$5\%CO_2$. The medium was then replaced with reoxygenation medium, and cells were further incubated at 37°C in a $95\%O_2$-$5\%CO_2$ atmosphere for 8h. Cells were processed for immunofluorescence staining (YAP, Cell Signaling Technology), caspase-3/7 detection (CellEvent caspase-3/7 detection; ThermoFisher) and JC-1 assay (MitoProbe JC-1 assay; ThermoFisher), and supernatants were assessed for ALT.

Hepatic stellate cells (HSCs) culture.

Mouse HSCs were isolated by *in situ* collagenase perfusion followed by Nycodenz gradient centrifugation from mice at 7days post IRI[25]. Immunofluorescence staining of YAP and α-SMA were processed 10h after planting.

Statistical analysis.

Group comparisons were performed using a Student's t test for mouse experiments, and Mann-Whitney U test was used for human data. Linear regression (R^2) was used to evaluate the strength of linear relationship between variables. P<0.05 was considered to be statistically significant.

Results

Post-OLT YAP expression negatively correlated with liver function and tissue damage in human OLT.

We first aimed to evaluate the peri-operative graft YAP expression and its correlation with liver damage in a human OLT cohort (n=60). Pre-OLT hepatic biopsies were collected during back-table preparation after 2-10h cold storage (prior to implantation) and post-OLT biopsies were obtained at 3h after reperfusion (prior to abdominal closure). Western blot-assisted pre- and post-OLT YAP expression profiles are shown in Fig. 1a (representative of 6 cases). As pre-OLT YAP was at basal level, post-OLT YAP expression increased after reperfusion. Interestingly, the post-OLT YAP levels correlated negatively with sALT values at POD1 (Fig.1b: R^2=0.1560, p=0.0018), indicating that increased post-OLT YAP expression was essential for hepatic cytoprotection. There was no significant correlation between post-OLT YAP ratio and cold ischemia time, or intraoperative blood loss (surgical stress factors, Suppl.Fig.1a).

To evaluate the impact of post-OLT YAP levels for clinical outcomes, sixty human OLTs were divided into low post-OLT YAP group (Low YAP: n=33) and high post-OLT YAP group (High YAP: n=27) by using post-OLT YAP/β-actin ratio=0.95 as threshold (Fig.1c). There was no significant correlation between post-OLT YAP classification and donor/ recipient background, e.g., cold ischemia time, MELD score, age, gender, weight/BMI or serum TG/Cholesterol values (Suppl.Table1, Suppl.Fiq.1b). Unlike Low YAP group, OLT recipients characterized by high post-OLT YAP levels exhibited lower sALT at POD1 (Fig. 1d, p<0.01), as well as rapid recovery of sALT from POD1 to POD7 (Fig.le). Moreover, post-OLT YAP expression in graft (green fluorescence indicative of YAP) negatively correlated with liver histology and hepatocellular death in liver biopsies (at 3h after portal reperfusion), as evidenced by H&E staining (pathologic features as sinusoidal congestion, edema, vacuolization were shown in Low YAP group), TUNEL staining (grey color indicative of necrosis/apoptosis in Low YAP group) and DHE staining (bright red fluorescence indicative of high intracellular oxidation in Low YAP group) (Fig. 1f).

Local YAP expression profile in murine liver IRI.

We then determined whether IR triggered the expression of endogenous YAP gene in mouse livers subjected to 90min of warm ischemia, followed by reperfusion. Unlike in sham controls, YAP mRNA levels increased progressively after the ischemia insult, peaking by 1-6h of reperfusion and decreasing thereafter (Fig.2a; p<0.001).

YAP activation ameliorated liver IRI.

We analyzed the hepatocellular damage after modulation of YAP pathway in our mouse model of 90min of warm ischemia followed by 6h of reperfusion. Treatment with YAP activator (LPA) at 1h prior to the onset of ischemia promoted YAP gene and protein induction (Fiq.2b.2e). Unlike in control PBS group, mice pre-treated with LPA were resistant to liver IRI, evidenced by reduced sALT levels (Fig.2c; p<0.001); and well-preserved hepatic architecture, without sinusoidal congestion, edema, vacuolization or necrosis (Fig.2d). To document the beneficial effect was YAP-dependent, a separate group of

WT mice was pre-treated with YAP inhibitor (VP). Compared to controls, YAP inhibition exacerbated liver IRI, evidenced by increased sALT levels (Fig.2c; $p<0.001$); and more severe lobular edema, widespread hemorrhage, congestion/hepatocellular necrosis (Fig.2d).

YAP activation attenuated oxidative stress in liver IRI.

To assess putative regulatory role of YAP activation, we screened IR-induced oxidative stress and hepatic oncotic necrosis/apoptosis. Pre-treatment with LPA activated Hippo pathway downstream regenerative (ctgf, cyr61, ankrd1) and anti-oxidative (MnSOD, catalase) gene programs (Fig.2f; $p<0.001$), decreased intracellular oxidative stress (DHE staining: no red fluorescence; Fig.3a), prevented hepatocellular necrosis/apoptosis and reduced frequency of TUNEL^{+} cells (Fig.3b: red arrow; Suppl.Fig.2a). By targeting YAP-TEAD signaling[21], pretreatment with VP diminished ($p<0.001$) downstream gene induction (ctgf, cyr61, ankrd1, MnSOD, catalase; Fig.2f). Strikingly, VP-assisted YAP inhibition significantly enhanced liver oxidative stress (DHE staining: intensive red fluorescence indicative of ROS production, Fig.3a) and hepatocellular necrosis/apoptosis (increased frequency of TUNEL^{+} cells, Fig.3b: red arrow; Suppl.Fig.2a).

YAP activation diminished innate immune response in liver IRI.

LPA-facilitated YAP activation suppressed macrophages (CD68^{+}) and neutrophils (Ly6G^{+}) infiltration (Fig.3c: white arrow; Suppl.Fig.2b), and abolished pro-inflammatory cytokine expression pattern (Fig.3d: TNF-α, IL-1β, IL-6, $p<0.001$). In contrast, YAP inhibition amplified macrophage/neutrophil sequestration (Fig.3c: white arrow; Suppl.Fig.2b), and increased cytokine expression (Fig.3d: TNF-α, IL-1β, IL-6, $p<0.001$).

YAP activation prevented hepatocyte death.

We then analyzed the modulatory function of YAP activation in well-controlled hypoxia-reoxygenation stressed mouse primary hepatocyte cultures. LPA treatment enhanced YAP accumulation in hepatocyte nucleus (Fig.4c: red fluorescence indicated positive YAP in nucleus, Suppl.Fig.2c), promoted downstream regenerative/anti-oxidative gene expression (Fig.4a: ctgf, cyr61, ankrd1 and MnSOD) and protected hepatocytes against oxidative stress, as evidenced by decreased ALT release (Fig.4b), less caspase-3/7 activity (Fig.4d, green fluorescence indicative of positive caspase-3/7 in nucleus, Suppl.Fig.2c), and intact mitochondria membrane (Fig.4e: JC-1 staining: red fluorescence indicative of less mitochondria depolarization, Suppl. Fig.2c), as compared with control group. In contrast, VP facilitated YAP depression in hepatocytes nucleus (Fig.4c, Suppl.Fig.2c) and suppressed YAP downstream gene induction (Fig.4a). As VP mainly blocked the YAP–TEAD axis, basal level of YAP was observed in cytoplasm (Fig.4c, Suppl.Fig.2c). VP mediated YAP inhibition further exacerbated hepatocellular damage, as shown by higher ALT release (Fig. 4b), abundant caspase-3/7 activity (Fig.4d, Suppl.Fig.2c), and ROS-stressed mitochondria (Fig.4e: JC-1 staining: green fluorescence indicative of mitochondria depolarization, Suppl.Fig.2c).

YAP activation abolished liver IR-mediated fibrosis.

Although serum ALT levels progressively decreased from 6h to 1d post-reperfusion in IR-stressed livers, and returned to normal by 3d (Fig.5a), liver fibrosis was steadily developing from 1d to 7d, as shown by gross morphology (fibrotic change), H&E staining (fibrous portal expansion and aggregated collagen fibers), Masson's trichrome staining (blue color was indicative of collagen deposition), and Sirius red staining (red color was indicative of collagen deposition) (Fig.5b, Suppl.Fig.2d,3a). Interestingly, IR-stressed livers in mice pre-treated with LPA maintained intact hepatic architecture, diminished fibrosis formation during the recovery (Fig.5b, Suppl.Fig.2d,3b), and suppressed ECM synthesis (Fig.5c: α-SMA, Col1a1 and TIMP1, p<0.001). In contrast, VP pre-treatment delayed liver recovery despite serum ALT returning to normal levels by 7d (Fig.5a), as evidenced by severe fibrosis (Fig.5b, Suppl.Fig.2d,3c: expanded necrosis area, severe inflammatory infiltration, aggressive collagen deposition around portal areas), and enhanced fibrosis-related gene expression program (Fig.5c).

YAP inhibition potentiated hepatic stellate cell stimulation.

Stimulation of HSCs is responsible for ECM deposition and fibrosis development[9]. VP treatment elevated TGF-β and pro-inflammatory cytokines (TNF-α, IL-1β, IL-6) in IR-livers from 6h to 7d post-reperfusion (Fig.6a). We then cultured HSCs harvested from ischemic livers at 7d post-reperfusion. Interestingly, HSCs from VP-treated livers were fibrogenic and contractile with abundant YAP and α-SMA, while LPA-treated with of rounded shape and minimal YAP and α-SMA levels (Fig.6b: green color indicative of YAP while red color indicative of α-SMA expression). We also found increased α-SMA expression in VP-treated liver, as compared with the LPA-conditioned group using *in vivo* α-SMA immunofluorescence staining (Fig.6c: red color indicative of α-SMA expression).

Nrf2 is required for LPA facilitated hepatocellular protection in liver IRI.

Given the previously defined anti-oxidative role of Nrf2 in IRI[26], we then determined the hepatocellular damage after infusion of YAP activator in Nrf2-deficient mice subjected to 90min of warm ischemia followed by 6h of reperfusion. As LPA treatment, but not VP induced hepatic Nrf2 protein expression in WT liver IRI (Fig.7a), LPA administration failed to prevent liver IRI in Nrf2-deficient mice, indicated by comparable sALT levels (Fig.7b) and elevated gene induction of pro-inflammatory cytokine profiles (Fig.7c). Consistent with *in vivo* findings, LPA failed to protect Nrf2-deficient hepatocvtes against hypoxia-reoxygenation stress (Fig.8a,8b,8c). It may imply that YAP mediated hepatocellular protection was Nrf2 dependent. After 7d of reperfusion, both LPA and control groups in Nrf2-deficient mice represented massive fibrosis development, as shown by gross morphology (fibrotic change), H&E staining (fibrous portal expansion and aggregated collagen fibers), Masson's trichrome staining (dense blue color indicated collagen deposition), and Sirius red staining (dense red color indicated collagen deposition) (Fig.7d, Suppl.Fig.2e). HSCs from LPA-treated Nrf2-deficient livers were fibroqenic/contractile with abundant YAP and α-SMA (Fig.8d : green color indicative of YAP while red color indicative of α-SMA expression).

Discussion

The present study is the first to demonstrate post-OLT YAP expression in human liver transplants correlated with clinical outcomes. Indeed, high perioperative YAP expression was accompanied by better preserved liver histopathology and hepatocellular function in OLT recipients. Our parallel study in well-established murine liver IRI model revealed the crucial role of YAP signaling in hepatocellular protection and HSCs mediated fibrosis *in vivo* and *in vitro.* As liver IR triggered endogenous local YAP induction, a single intravenous infusion of LPA, a YAP activator, conferred hepatic cytoprotection against IR insult, evidenced by diminished sALT levels, reserved hepatic architecture, amplified regenerative/anti-oxidative gene program, attenuated hepatocellular necrosis/apoptosis, and abolished innate immune responses. These findings were confirmed in hypoxia-reoxygenation stressed primary mouse hepatocyte cultures, where activation of YAP ameliorated cellular damage and necrosis/apoptosis by augmenting regenerative/anti-oxidative gene programs. As IR-activated HSCs contribute to liver fibrosis, YAP inhibition exacerbated the hepatocellular damage to enhance HSCs activation, which resulted in prolonged recovery and massive fibrosis. However, YAP activation prevented IRI, which suspended HSCs activity and ultimate fibrogenesis. Interestingly, LPA, YAP activator, failed to protect liver against IR insult, and resulted in massive fibrosis in Nrf2-deficient mice.

Hence, this translational study highlights the pivotal modulatory role of YAP pathway in combating IR-hepatocellular damage, and maintaining homeostasis in IR-stressed OLTs.

In the clinical arm of our study, post-OLT YAP expression was dramatically increased in 45% (27/60, post-OLT YAP/β-actin>0.95) of human OLTs (exclusion of fatty liver. Suppl.Fig.1b). which associated with well-preserved liver histology and improved hepatocellular function. It may imply that YAP signaling is required for self-repair and homeostasis maintenance under the cellular stress. In agreement with human data, we first found that warm ischemia insult triggered hepatic endogenous YAP expression in mouse liver, the levels of which were elevated between 1-6h of reperfusion (damage phase). It is plausible that YAP induction progresses in parallel with IR-mediated hepatocellular damage. To mimic liver IRI *in vivo*, we employed hypoxia-reoxygenation stressed primary hepatocyte cultures in which cellular stress mediated intrinsic accumulation of YAP in hepatocyte nucleus. Strikingly, enhancement of YAP by exogenous LPA attenuated liver IRI, evidenced by diminished sALT levels and well-preserved histology in WT mice, while promoting nuclear YAP production to protect hepatocytes against hypoxia-reoxygenation stress *in vitro.* In marked contrast, treatment with YAP inhibitor abolished regenerative/anti-oxidative gene expression programs, exacerbated hepatic IRI, and potentiated hypoxia-reoxygenation mediated hepatocellular damage *in vitro.*

Liver IRI combines two phases of ischemia-trigged hypoxic cellular stress, and inflammation-mediated reperfusion injury. Endogenous ROS-inflicted tissue damage initiates circulatory disturbances and cascade of inflammation responses, leading to the hepatocyte death[1“3]. Hepatocyte oncotic necrosis and apoptosis, which render parenchymal cytodestruction, proceed via DNA degradation detected by TUNEL assay[27]. We observed mild positive TUNEL^{+} cells and moderate red DHE staining in Low YAP group in human

OLTs, which is consistent with relatively high post-OLT sALT levels. To further evaluate the putative role of YAP in liver IRI, we demonstrated that YAP activation facilitated downstream regenerative (ctgf, cyr61, and ankrd1) and anti-oxidative (MnSOD and catalase) gene programs, diminished ROS production (DHE staining: no red color), abolished hepatocyte oncotic necrosis/apoptosis (very low frequency of TUNEL+ cells), and decreased CD68+ macrophage/Ly6G+ neutrophil infiltration and function (IRI signature markers, i.e., TNF-α, IL-1β and IL-6). Conversely, VP-assisted YAP inhibition enhanced hepatic ROS production (DHE staining: dense red color), increased frequency of TUNEL+ cells and augmented CD68+ macrophage/Ly6G+ neutrophil hepatic sequestration and pro-inflammatory cytokine expression. It is plausible that YAP activation prevents hepatocellular damage by enhancing hepatocellular regeneration and anti-oxidation activity while maintaining hepatocyte integrity against oncotic necrosis and apoptosis. We have previously documented TIM-4+ macrophage mediated hepatocyte phagocytosis was the initial stimulus of innate immunity in liver IRI[3]. Here, YAP activation prevented hepatocellular damage, which further abolished innate immune responses in liver IRI. In agreement with our *in vivo* data, YAP activation ameliorated ALT release, diminished hepatocyte death, and maintained mitochondrial integrity in hypoxia-reoxygenation insulted primary hepatocyte cultures. These results reinforce the critical role of YAP in promoting hepatocellular anti-oxidation and regeneration against IR-insult, with resultant improvement of liver function. Furthermore, YAP inhibition exacerbated hepatocyte death, confirming this regulation at hepatocyte level was YAP dependent.

Fibrosis after liver transplantation is associated with impaired liver function and poor graft survival[5,7,28]. Acute liver injury also leads to fibrosis, which is considered as an attempt to repair damaged tissue and trigger self-limited protection[29]. In our study, inhibiting YAP resulted in delayed post-IRI liver recovery, while triggering abundant ECM synthesis (α-SMA, Col1a1 and TIMP1), massive collagen deposition and fibrosis development. It has been shown that monocyte-derived macrophages are the predominant pro-fibrogenic macrophage population in the liver[30]. In fibrotic liver, macrophages were found consistently localizing in close proximity to activated myofibroblasts while their depletion attenuated carbon tetrachloride (CCl4) inflicted liver fibrosis[31,32]. TGF-β, produced by macrophages, activated myofibroblast, as well as promoted ECM synthesis[33,34]. Recent study showed that macrophage-derived pro-inflammatory TNF-α and IL-1β were essential to maintain myofibroblast survival through nuclear factor kB (NF-kB)[13,14]. Here, we found that the severity of IR-mediated liver fibrosis increased along with the hepatocellular damage. Indeed, YAP activation prevented hepatocyte damage in liver IRI with minimal fibrosis and suppressed macrophage function. On the other hand, YAP inhibition exerted opposite effects, i.e., exacerbated IR-hepatocyte, associated with amplified macrophage pro-inflammatory cytokine expression (TNF-α, I L-1β and IL-6) between 6h and 7d of reperfusion. In addition, TGF-β was further enhanced, along with fibrogenesis development.

Fate tracing has revealed that HSCs are dominant contributors to liver fibrosis, regardless of the etiology[9]. Stimulated by pro-inflammatory cytokines (TGF-β, TNF-α, IL-1β and IL-6), HSCs become activated and transdifferentiate to myofibroblast cells, which are characterized by loss of lipid droplets, increased migration and excessive ECM synthesis[25]. Recent study has shown that VP-mediated YAP inhibition attenuated HSCs activity in liver

IRI[35]. In our murine liver IRI model, HSCs were activated and transferred to myofibroblasts, along with hepatic pro-inflammatory cytokine induction at very early post-reperfusion stage (6h). Recent studies have shown that YAP was a core regulator in HSCs activation/ differentiation into myofibroblasts[36,37]. Upregulating YAP in HSCs/myofibroblasts prolonged their activation and promoted ECM synthesis, which led to more severe fibrosis[36,37]. Intriguingly, we found that YAP activation largely protected IR-stressed hepatocytes, with reduced pro-inflammation and HSCs inactivation. Unlike hepatocytes, quiescent HSCs were insensitive to YAP activation (Suppl.Fig.4), which resulted in minimal liver fibrosis. On the other hand, YAP inhibition exacerbated hepatocyte damage, with abundant pro-inflammatory response, HSCs activation, and liver fibrogenesis. These results imply that HSCs-mediated liver fibrosis requires two signals: (1)initial stimulus to quiescent HSCs by IR-induced pro-inflammatory cytokines; (2)regulation by YAP activation.

The transcription factor Nrf2, regulating cellular resistance against oxidative stress, has been considered as a "master switch" of intracellular redox homeostasis[38]. We have shown that Nrf2-deficient liver grafts were susceptible to IR-mediated damage[26]. It has been shown that crosstalk between Nrf2 and YAP facilitated anti-oxidation in bladder cancer cells[39]. Interestingly, LPA infusion, but not VP preferentially heighten Nrf2 protein production in IR-stressed WT livers. By employing Nrf2-deficient mice, we further determined that LPA administration failed to protect liver against IR-damage, as evidenced by raised sALT levels and abundant innate immune response. YAP activation also failed to attenuate IR-mediated fibrogenesis in Nrf2-deficient mice. Hence, Nrf2 signaling is required for YAP activation mediated cytoprotection in liver IRI.

In summary, this study systemically evaluated the pivotal role of YAP in hepatic protection and fibrosis development in liver IRI. Harnessing cytoprotective and fibrogenesis mechanisms by YAP may be essential in the maintenance of hepatic homeostasis *in vivo* by minimizing local organ damage and depressing HSCs-dependent fibrosis. As YAP-mediated hepatocellular protection and fibrosis induction was Nrf2-dependent, our findings provide new insights into the pathogenesis of, and identify potential novel molecular targets for therapeutic intervention against sterile inflammatory liver damage and fibrosis.

Supplementary Material

Refer to Web version on PubMed Central for supplementary material.

Acknowledgments

References

1. Ji H, Shen X, Gao F et al. Programmed death-1/B7-H1 negative costimulation protects mouse liver against ischemia and reperfusion injury. Hepatology 2010;52:1380–1389. [PubMed: 20815020]

2. Ji H, Zhang Y, Shen X et al. Neuropeptide PACAP in mouse liver ischemia and reperfusion injury: Immunomodulation by the cAMP-PKA pathway. Hepatology 2013;57:1225–1237. [PubMed: 22532103]

3. Ji H, Liu Y, Zhang Y et al. T-cell immunoglobulin and mucin domain 4 (TIM-4) signaling in innate immune-mediated liver ischemia-reperfusion injury. Hepatology 2014;60:2052–2064. [PubMed: 25066922]

4. Duffy JP, Kao K, Ko CY et al. Long-term patient outcome and quality of life after liver transplantation: analysis of 20-year survivors. Ann Surg 2010;252:652–661. [PubMed: 20881772]

5. Evans HM, Kelly DA, McKiernan PJ et al. Progressive histological damage in liver allografts following pediatric liver transplantation. Hepatology 2006;43:1109–1117. [PubMed: 16628633]

6. Ekong UD, Melin-Aldana H, Seshadri R et al. Graft histology characteristics in long-term survivors of pediatric liver transplantation. Liver Transpl 2008;14:1582–1587. [PubMed: 18975292]

7. Scheenstra R, Peeters PM, Verkade HJ et al. Graft fibrosis after pediatric liver transplantation: ten years of follow-up. Hepatology 2009;49:880–886. [PubMed: 19101912]

8. Schuppan D, Afdhal NH. Liver cirrhosis. Lancet 2008;371:838–851. [PubMed: 18328931]

9. Mederacke I, Hsu CC, Troeger JS et al. Fate tracing reveals hepatic stellate cells as dominant contributors to liver fibrosis independent of its aetiology. Nat Commun 2013;4:2823. [PubMed: 24264436]

10. Martin K, Pritchett J, Llewellyn J et al. PAK proteins and YAP-1 signalling downstream of integrin beta-1 in myofibroblasts promote liver fibrosis. Nat Commun 2016;7:12502. [PubMed: 27535340]

11. Gabbiani G The myofibroblast in wound healing and fibrocontractive diseases. J Pathol 2003;200:500–503. [PubMed: 12845617]

12. Ide M, Kuwamura M, Kotani T et al. Effects of gadolinium chloride (GdCI(3)) on the appearance of macrophage populations and fibrogenesis in thioacetamide-induced rat hepatic lesions. J Comp Pathol 2005;133:92–102. [PubMed: 15964588]

13. Sunami Y, Leithauser F, Gul S et al. Hepatic activation of IKK/NFkappaB signaling induces liver fibrosis via macrophage-mediated chronic inflammation. Hepatology 2012;56:1117–1128. [PubMed: 22407857]

14. Pradere JP, Kluwe J, Minicis S et al. Hepatic macrophages but not dendritic cells contribute to liver fibrosis by promoting the survival of activated hepatic stellate cells in mice. Hepatology 2013;58:1461–1473. [PubMed: 23553591]

15. Yimlamai D, Christodoulou C, Galli GG et al. Hippo pathway activity influences liver cell fate. Cell 2014;157:1324–1338. [PubMed: 24906150]

16. Dong J, Feldmann G, Huang J et al. Elucidation of a universal size-control mechanism in Drosophila and mammals. Cell 2007;130:1120–1133. [PubMed: 17889654]

17. Yagi R, Chen LF, Shigesada K et al. A WW domain-containing yes-associated protein (YAP) is a novel transcriptional co-activator. EMBO J. 1999;18:2551–2562. [PubMed: 10228168]

18. Lee DH, Park JO, Kim TS et al. LATS-YAP/TAZ controls lineage specification by regulating TGFbeta signaling and Hnf4alpha expression during liver development. Nat Commun 2016;7:11961. [PubMed: 27358050]

19. Torre C, Perret C, Colnot S. Molecular determinants of liver zonation. Prog Mol Biol Transl Sci 2010;97:127–150. [PubMed: 21074732]

20. Kim W, Khan SK, Gvozdenovic-Jeremic J et al. Hippo signaling interactions with Wnt/beta-catenin and Notch signaling repress liver tumorigenesis. J Clin Invest 2017;127:137–152. [PubMed: 27869648]

21. Zhang N, Bai H, David KK et al. The Merlin/NF2 tumor suppressor functions through the YAP oncoprotein to regulate tissue homeostasis in mammals. Dev Cell 2010;19:27–38. [PubMed: 20643348]

22. Zhou D, Conrad C, Xia F et al. Mst1 and Mst2 maintain hepatocyte quiescence and suppress hepatocellular carcinoma development through inactivation of the Yap1 oncogene. Cancer cell 2009;16:425–438. [PubMed: 19878874]

23. Grijalva JL, Huizenga M, Mueller K et al. Dynamic alterations in Hippo signaling pathway and YAP activation during liver regeneration. Am J Physiol Gastrointest Liver Physiol 2014;307:G196–204. [PubMed: 24875096]

24. Kowalik MA, Saliba C, Pibiri M et al. Yes-associated protein regulation of adaptive liver enlargement and hepatocellular carcinoma development in mice. Hepatology 2011;53:2086–2096. [PubMed: 21391223]

25. Mederacke I, Dapito DH, Affo S et al. High-yield and high-purity isolation of hepatic stellate cells from normal and fibrotic mouse livers. Nat Protoc 2015;10:305–315. [PubMed: 25612230]

26. Ke B, Shen X, Zhang Y et al. KEAP1-NRF2 complex in ischemia-induced hepatocellular damage of mouse liver transplants. J Hepatol 2013;59:1200–1207. [PubMed: 23867319]

27. Jaeschke H, Lemasters JJ. Apoptosis versus oncotic necrosis in hepatic ischemia/reperfusion injury. Gastroenterology 2003;125:1246–1257. [PubMed: 14517806]

28. Berenguer M, Schuppan D. Progression of liver fibrosis in post-transplant hepatitis C: mechanisms, assessment and treatment. J Hepatol 2013;58:1028–1041. [PubMed: 23262248]

29. Dechene A, Sowa JP, Gieseler RK et al. Acute liver failure is associated with elevated liver stiffness and hepatic stellate cell activation. Hepatology 2010;52:1008–1016. [PubMed: 20684020]

30. Tacke F, Zimmermann HW. Macrophage heterogeneity in liver injury and fibrosis. J Hepatol 2014;60:1090–1096 [PubMed: 24412603]

31. Duffield JS, Forbes SJ, Constandinou CM et al. Selective depletion of macrophages reveals distinct, opposing roles during liver injury and repair. J Clin Invest 2005;115:56–65. [PubMed: 15630444]

32. Fallowfield JA, Mizuno M, Kendall TJ et al. Scar-associated macrophages are a major source of hepatic matrix metalloproteinase-13 and facilitate the resolution of murine hepatic fibrosis. J Immunol 2007;178:5288–5295. [PubMed: 17404313]

33. Hellerbrand C, Stefanovic B, Giordano F et al. The role of TGFβ1 in initiating hepatic stellate cell activation in vivo. J Hepatol 1999;30:77–87. [PubMed: 9927153]

34. Seki E, De Minicis S, Osterreicher CH et al. TLR4 enhances TGF-beta signaling and hepatic fibrosis. Nat Med 2007;13:1324–1332. [PubMed: 17952090]

35. Konishi T, Schuster RM, Lentsch AB. Proliferation of hepatic stellate cells, mediated by YAP and TAZ, contributes to liver repair and regeneration after liver ischemia-reperfusion injury. Am J Physiol Gastrointest Liver Physiol 2018;314:G471–482. [PubMed: 29351389]

36. Piersma B, de Rond S, Werker PM et al. YAP1 Is a driver of myofibroblast differentiation in normal and diseased fibroblasts. Am J Pathol 2015;185:3326–3337. [PubMed: 26458763]

37. Mannaerts I, Leite SB, Verhulst S et al. The Hippo pathway effector YAP controls mouse hepatic stellate cell activation. J Hepatol 2015;63:679–688. [PubMed: 25908270]

38. Ma Q Role of nrf2 in oxidative stress and toxicity. Annu Rev Pharmacol Toxicol 2013;53:401–426. [PubMed: 23294312]

39. Ciamporcero E, Daga M, Pizzimenti S et al. Crosstalk between Nrf2 and YAP contributes to maintaining the antioxidant potential and chemoresistance in bladder cancer. Free Radic Biol Med 2018;115:447–457. [PubMed: 29248722]

Highlights

- High graft YAP expression was correlated with well-preserved histology and improved hepatocellular function in human OLT

- Activating YAP promoted downstream regenerative/anti-oxidative gene induction, diminished oxidative stress and necrosis/apoptosis, and suppressed innate inflammation response in mouse liver IRI.

- YAP activation suppressed extracellular matrix synthesis, diminished hepatic stellate cells activation, and abolished mouse liver fibrogenesis during 7d post-IRI.

- YAP activation failed to protect Nrf2-deficient mouse livers against IR-mediated tissue damage, leading to extensive fibrosis at 7d post-IRI.
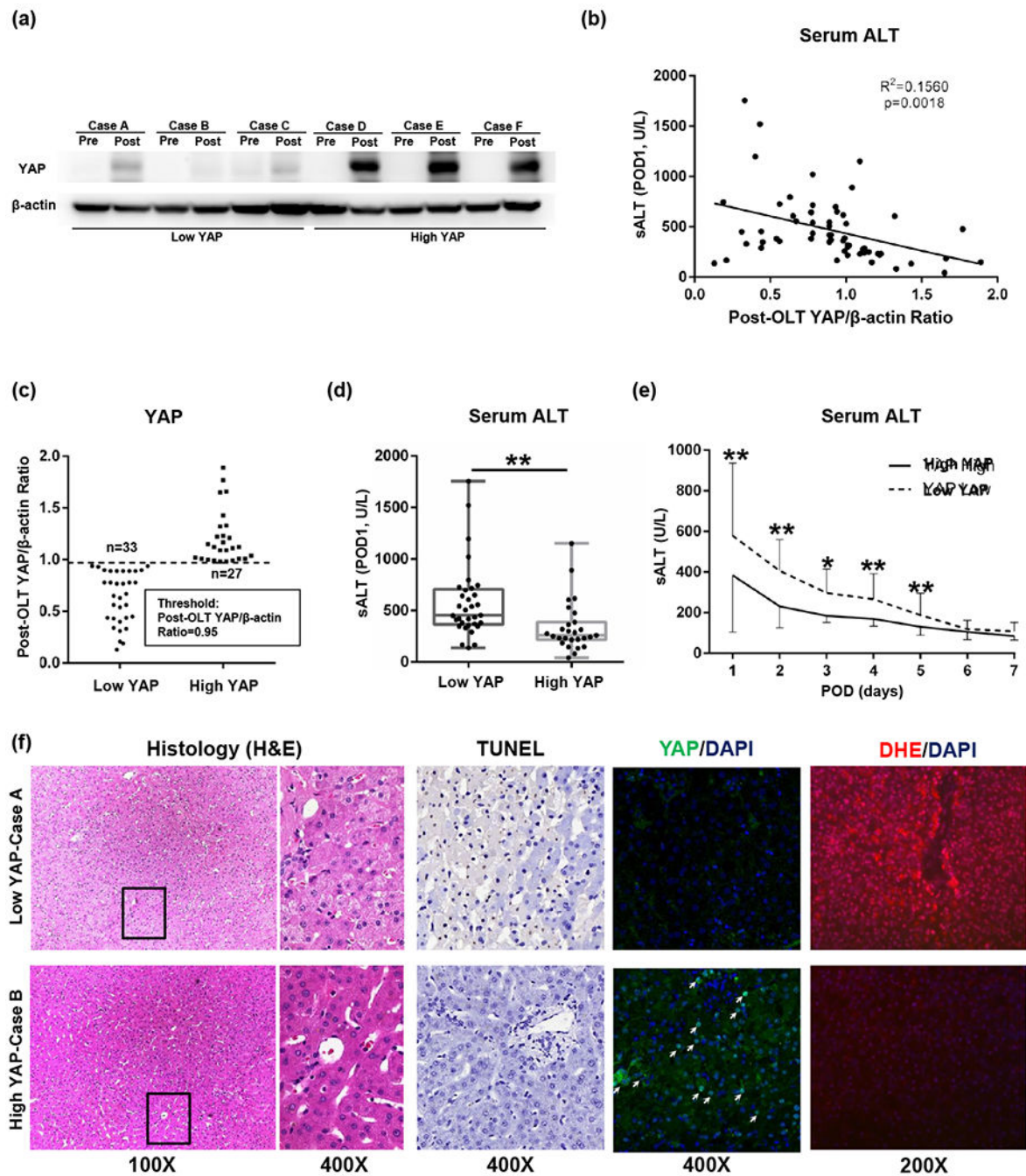
Fig.1.

Peri-operative hepatic YAP expression and its correlation with liver damage in human OLT (n=60). (a)Western blot-assisted pre- and post-OLT YAP expression profiles in OLT biopsies (representative 6 cases). (b)The ratio of post-OLT YAP/β-actin correlated negatively with sALT at POD1. (c)Sixty human OLTs were divided into low ratio of post-OLT YAP/β-actin group (Low YAP: n=33) and high ratio of post-OLT YAP/β-actin group (High YAP: n=27) by using post-OLT YAP/β-actin ratio=0.95 as threshold. (d)sALT values in both Low YAP and High YAP groups in OLT recipients at POD1. (e)sALT decreasing curve in Low YAP

and High YAP groups in OLT recipients (POD1-7). (f)Histology (H&E staining), TUNEL staining, YAP staining, DHE staining in OLT biopsies (representative 2 cases for Low YAP and High YAP groups) (magnification x100, x200 and x400; **p<0.01, *p<0.001 by Student's t test).
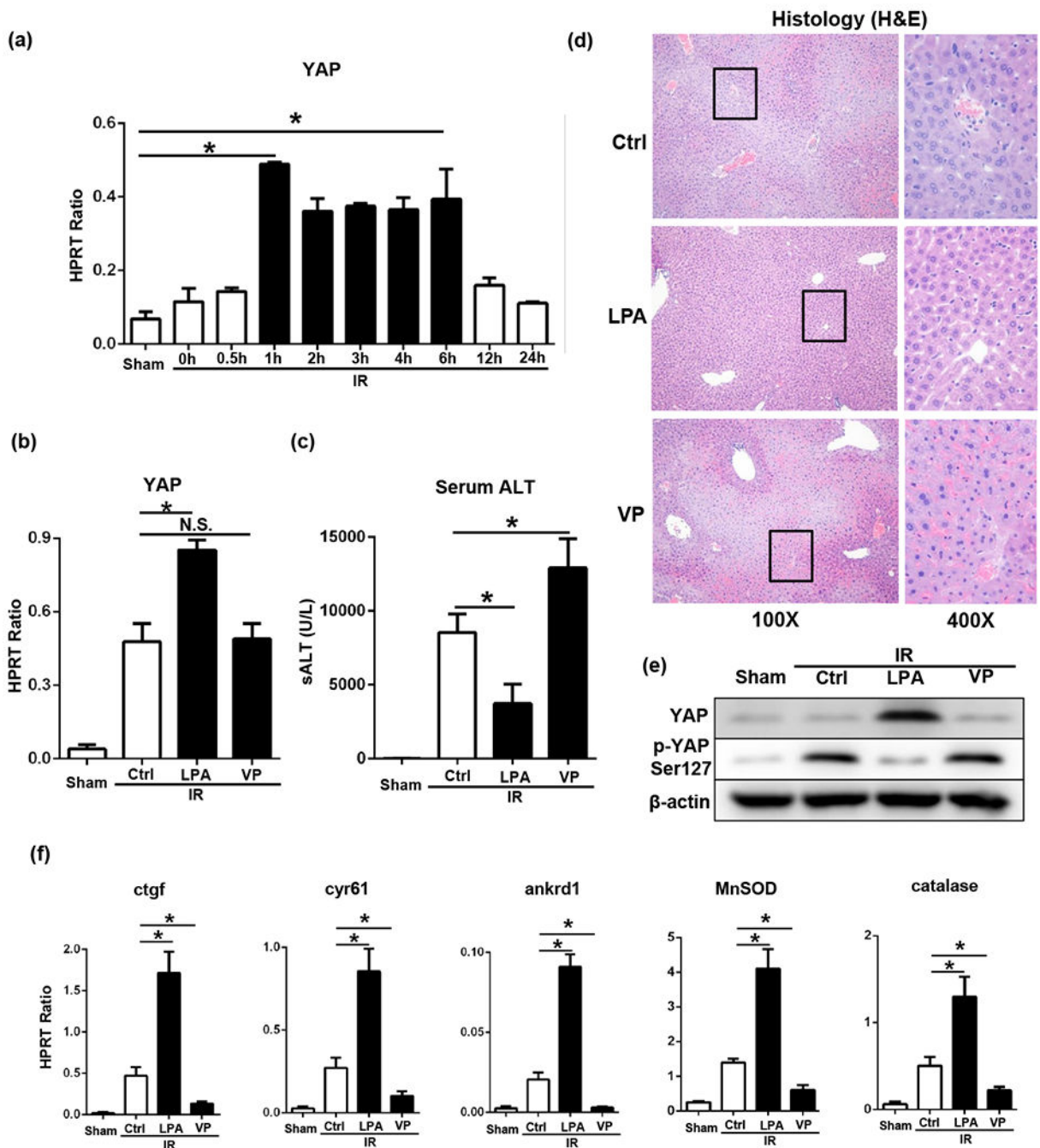
Fig.2.

(a)Kinetics of hepatic YAP gene expression in murine liver IRI. Liver samples harvested from B6 mice that were sham-operated or subjected to 90min of partial warm ischemia, followed by various lengths of reperfusion. WT mice were pre-treated with PBS (Ctrl, control), LPA (1-oleoyl lysophosphatidic acid, YAP activator) or VP (verteporfin, YAP inhibitor) at 1h before ischemia. Liver and serum samples were collected at 6h post reperfusion for: (b)YAP gene induction, (c)sALT levels, (d)liver histology (representative

H&E staining; magnification x100 and x400), (e)YAP and p-YAP(Ser127) protein induction and (f)YAP downstream gene expression (*p<0.001 by Student's t test; n=10-12/group).
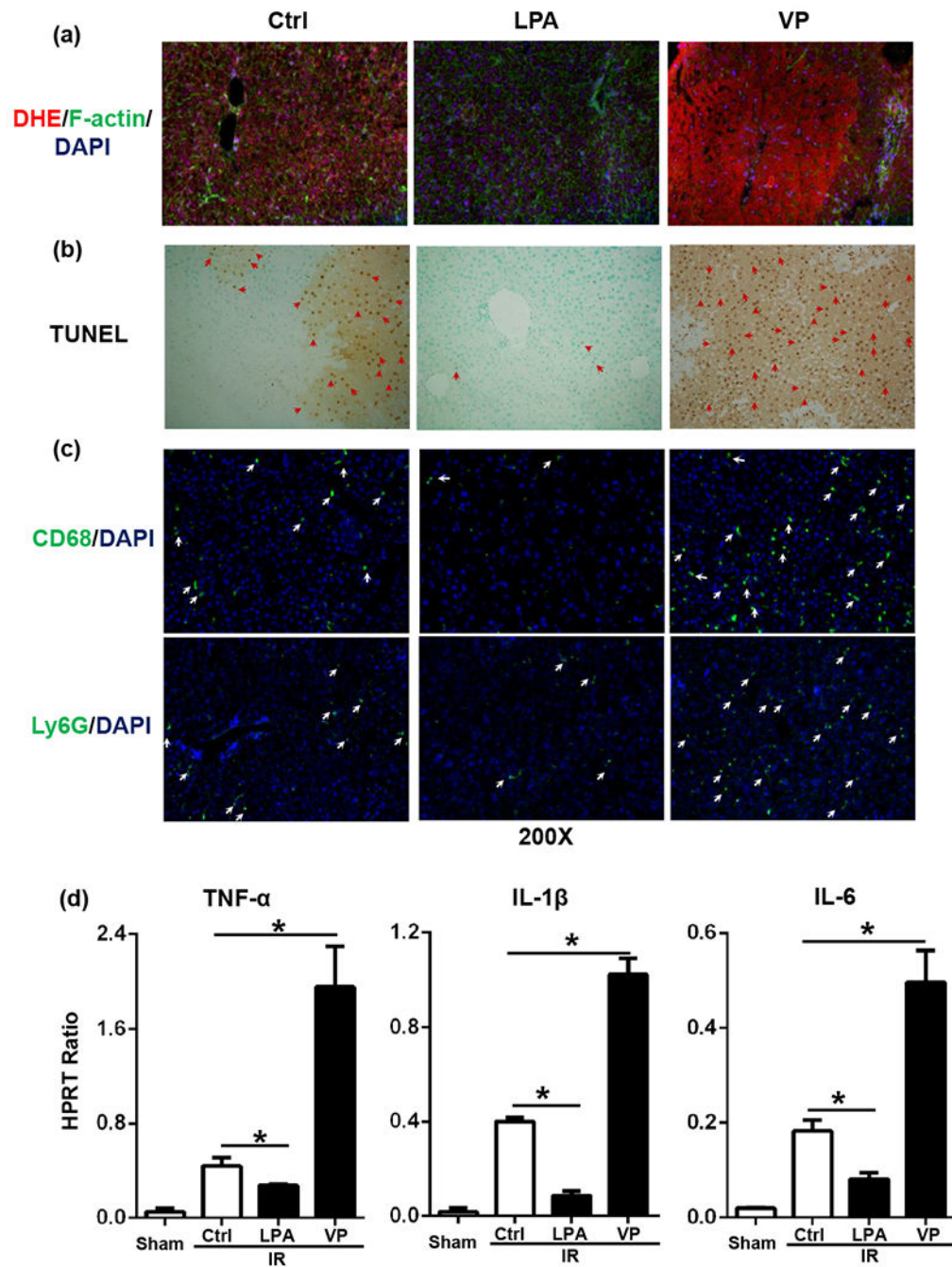
Fig.3.

YAP activation prevented hepatocyte death and suppressed pro-inflammatory response in liver IRI. Mice pre-treated with PBS, LPA or VP were subjected to 90min of warm ischemia, and analyzed at 6h of reperfusion for: (a)ROS-sensing dye dihydroethidium (DHE) staining (red fluorescence indicating ROS production). (b)TUNEL-assisted detection of hepatic necrosis/apoptosis (red arrows) in ischemic liver lobes. (c)CD68^{+} macrophages and Ly6G^{+} neutrophils in IR liver lobes (white arrow indicated positive staining). (d)qRT-PCR assisted

detection of TNF-α, IL-1β and IL-6 (magnification x200, *p<0.001 by Student's t test; n=4-6/group).
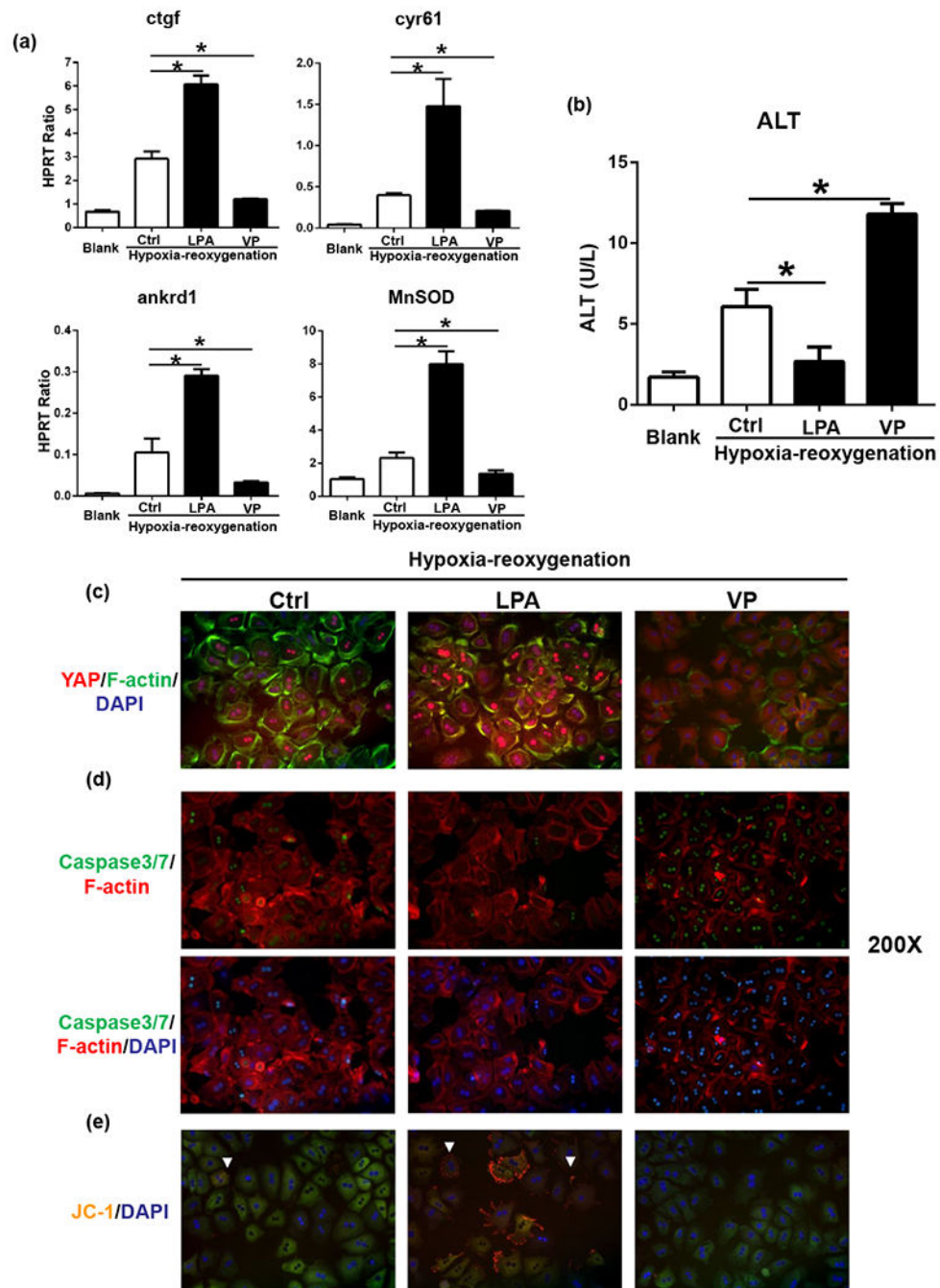
Fig.4.
YAP activation protected primary hepatocytes against hypoxia-reoxygenation insult i*n vitro.*
WT mouse hepatocyte cultures were supplemented with PBS, LPA or VP. After 6h of
hypoxia and 8h of reoxygenation, the cell cultures were analyzed for: (a)YAP downstream
gene expressions. (b)Supernatant ALT levels. (c)Hepatocellular YAP staining (red
fluorescence indicating YAP accumulation in nucleus). (d)Caspase-3/7 detection (green
fluorescence indicating positive caspase-3/7 in nucleus). (e)JC-1 staining (green

fluorescence indicating mitochondria depolarization, red fluorescence indicating intact mitochondria membrane) (magnification ×200, *p<0.001 by Student's t test; n=4-6/group).
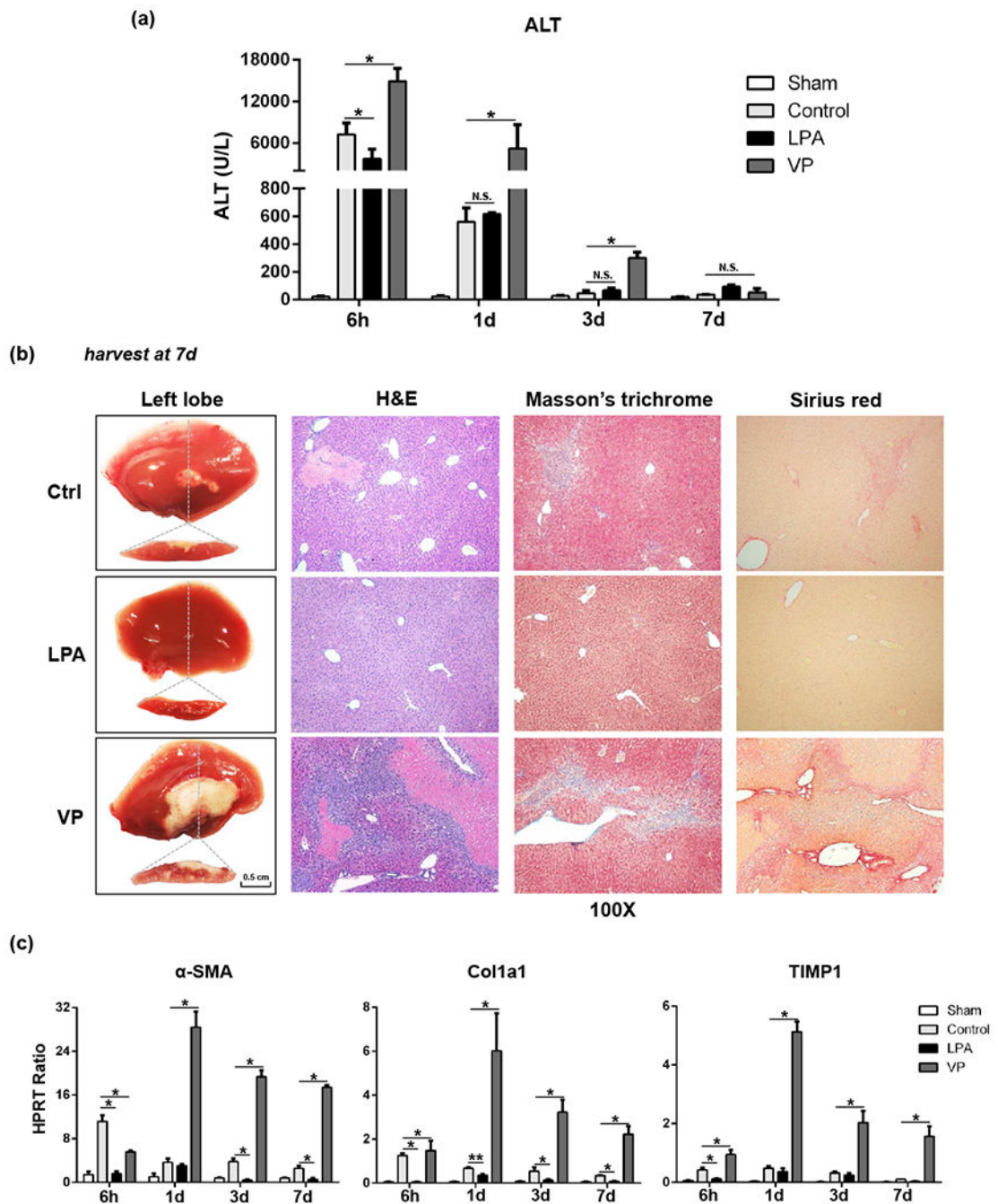
Fig.5.
YAP activation diminished fibrogenesis development after liver IRI. Mice pre-treated with PBS, LPA or VP were subjected to 90min of warm ischemia, followed by various lengths of reperfusion. Serum and liver samples were collected for: (a)ALT. (b)Histology (7d after reperfusion): gross morphology (fibrotic change); H&E staining; Masson's trichrome staining (blue color indicating collagen deposition); and Sirius red staining (red color indicating collagen deposition). (c)Fibrosis-related gene expression. (magnification x100, N.S. represented no significance, **p<0.01, *p<0.001 by Student's ttest; n=4-6/group).
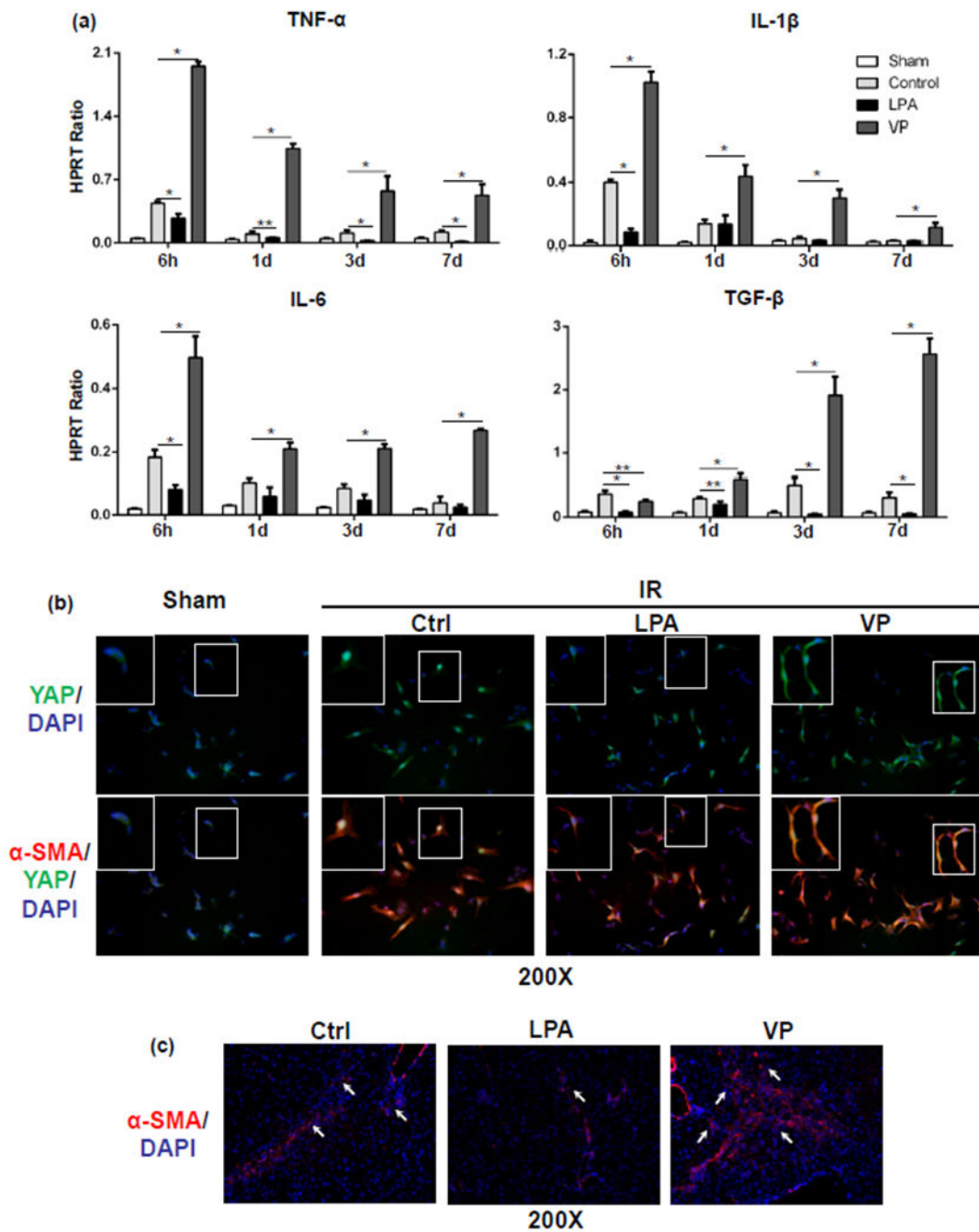
Fig.6.
YAP inhibition exacerbated inflammation and activated HSCs in liver IRI. Mice pre-treated with PBS, LPA or VP were subjected to 90min of warm ischemia, followed by various lengths of reperfusion. (a)Liver samples were harvested serially between 6h to 7d after reperfusion to measure pro-inflammatory cytokine gene inductions. (b)HSCs were isolated from IR-livers at 7d after reperfusion, and stained for YAP (green fluorescence) and α-SMA (red fluorescence). (c)IR-livers at 7d after reperfusion stained for α-SMA (red fluorescence) (magnification x200, **p<0.01, *p<0.001 by Student's ttest; n=4-6/group).
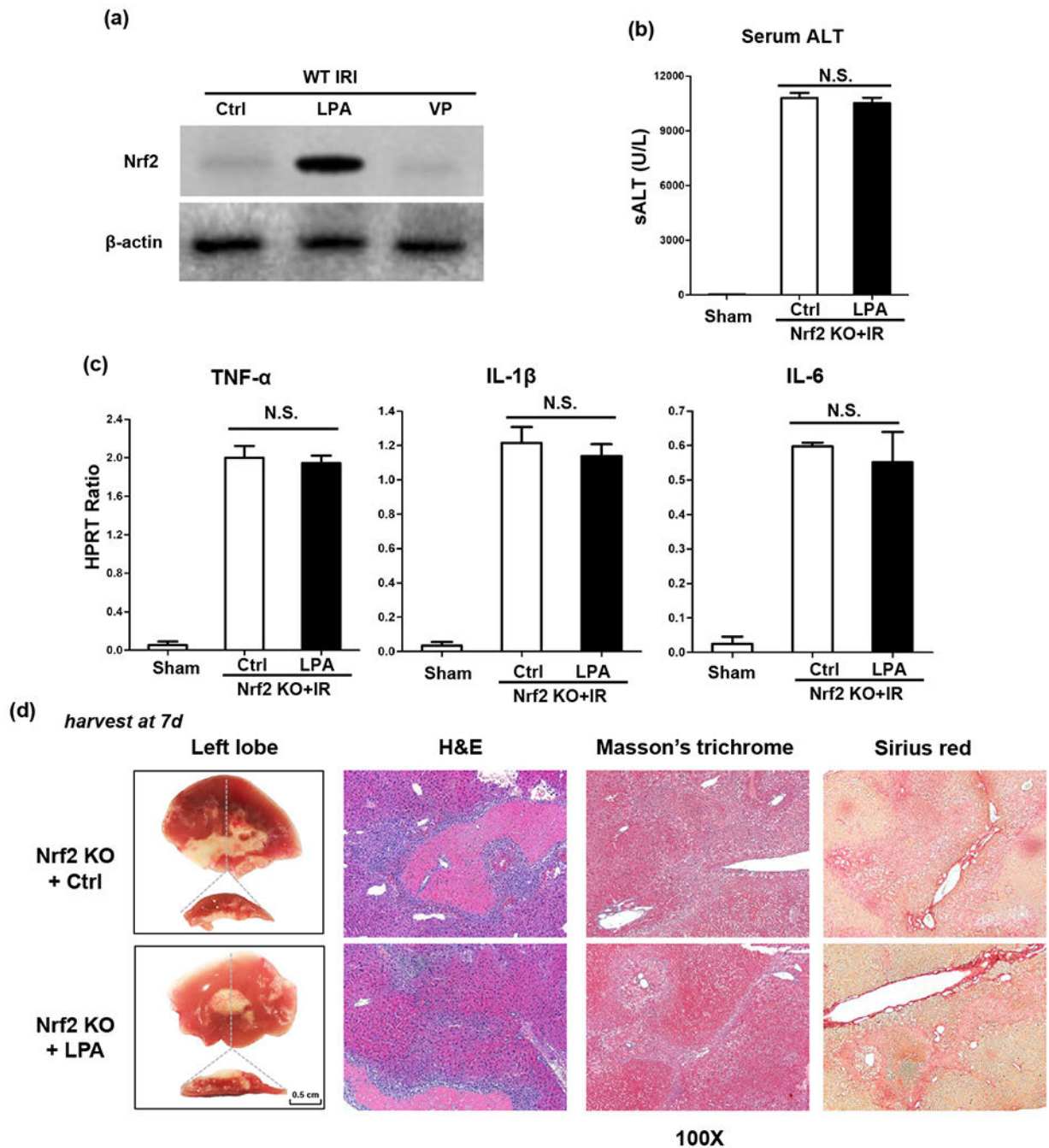
Fig.7.
YAP activation failed to protect Nrf2-deficient livers against IR-damage. WT and Nrf2-deficient mice pre-treated with PBS, LPA or VP were subjected to 90min of warm ischemia followed by 6h or 7d of reperfusion. Liver and serum samples were collected for analysis. (a)Western blot-assisted Nrf2 expression in WT liver after IRI. In Nrf2-deficient mice: (b)sALT levels. (c)qRT-PCR detected gene induction of TNF-α, IL-1β, IL-6. (d)Liver histology (7d after reperfusion): gross morphology (fibrotic change); H&E staining; Masson's trichrome staining (blue color indicating collagen deposition); and Sirius red

staining (red color indicating collagen deposition). (magnification x100, N.S. represented no significance by Student's t test; n=4-6/group).
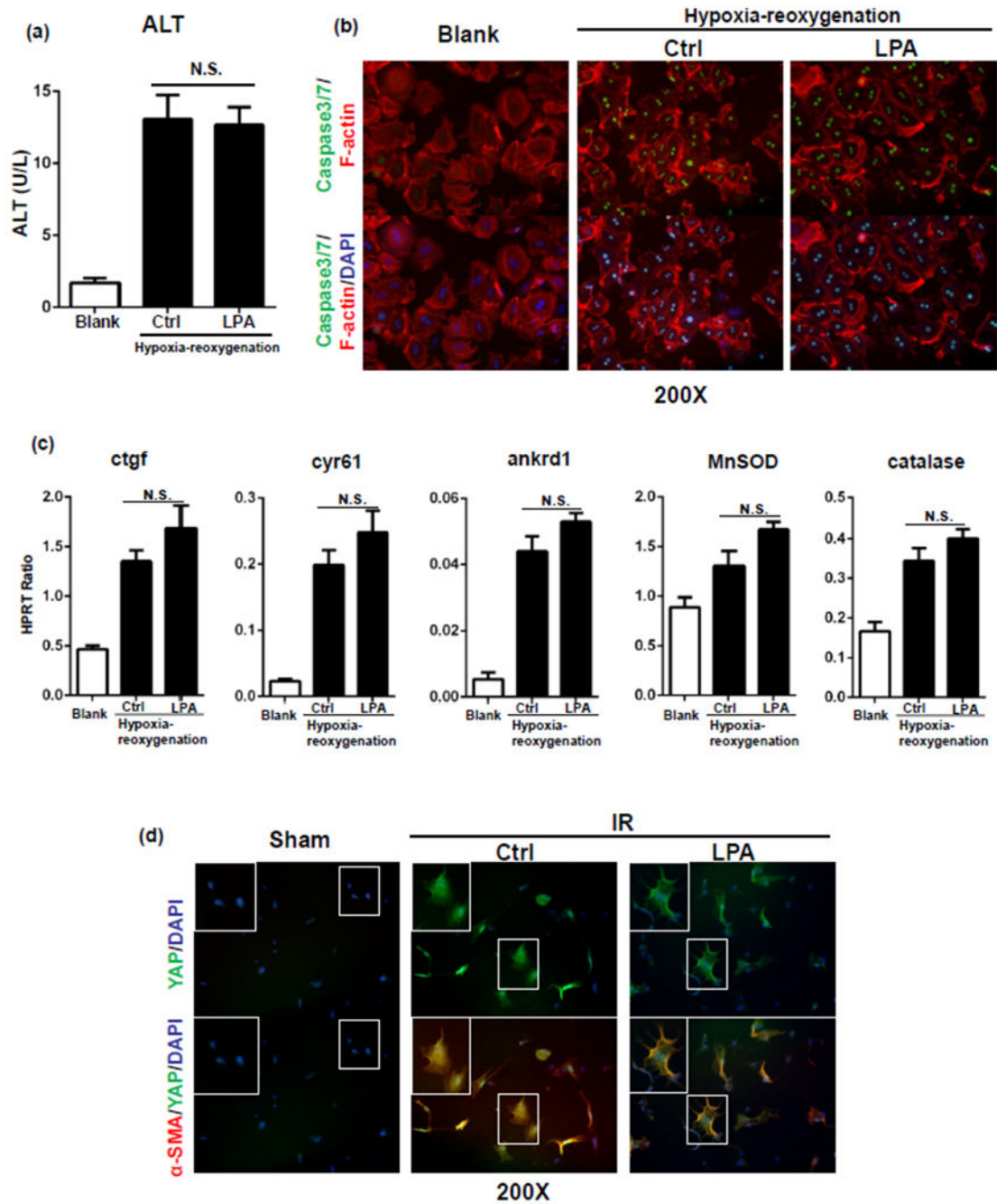
Fig.8.
YAP activation failed to protect Nrf2-deficient primary hepatocytes against hypoxia-reoxygenation insult *in vitro*, and failed to suppress Nrf2-deficient HSCs in liver IRI. Nrf2-deficient mouse hepatocyte cultures were supplemented with PBS or LPA. After 6h of hypoxia and 8h of reoxygenation, the cell cultures were analyzed for: (a)Supernatant ALT levels. (b)Caspase-3/7 detection (green fluorescence indicating positive caspase-3/7 in nucleus). (c)YAP downstream gene expressions. (d)HSCs were isolated from PBS or LPA treated IR-Nrf2-deficient livers at 7d after reperfusion, and stained for YAP (green

fluorescence) and α-SMA (red fluorescence). (magnification x200, N.S. represented no significance by Student's t test: n=4-6/qroup).